This article has been accepted for inclusion in a future issue of this journal. Content is final as presented, with the exception of pagination.

A New Microscopic Traffic Model Using a Spring-Mass-Damper-Clutch System

Zhaojian Li, Firas Khasawneh, Xiang Yin, Aoxue Li, and Ziyou Song

***Abstract*— Microscopic traffic models describe how cars interact with their neighbors in an uninterrupted traffic flow and are frequently used for reference in advanced vehicle control design. In this paper, we propose a novel mechanical system-inspired microscopic traffic model using a mass-spring-damper-clutch system. This model naturally captures the ego vehicle's resistance to large relative speed and deviation from a (driver- and speed-dependent) desired relative distance when following the lead vehicle. Compared with the existing car-following (CF) models, this model offers physically interpretable insights into the underlying CF dynamics and is able to characterize the impact of the ego vehicle on the lead vehicle, which is neglected in the existing CF models. Thanks to the nonlinear wave propagation analysis techniques for mechanical systems, the proposed model, therefore, has great scalability so that multiple mass-spring-damper-clutch systems can be chained to study the macroscopic traffic flow. We investigate the stability of the proposed model on the system parameters and the time delay using the spectral element method. We also develop a parallel recursive least square with inverse QR decomposition (PRLS-IQR) algorithm to identify the model parameters online. These real-time estimated parameters can be used to predict the driving trajectory that can be incorporated into advanced vehicle longitudinal control systems for improved safety and fuel efficiency. The PRLS-IQR is computationally efficient and numerically stable, and therefore, it is suitable for online implementation. The traffic model and the parameter identification algorithm are validated on both the simulations and naturalistic driving data from multiple drivers. Promising performance is demonstrated.**

***Index Terms*— Car-following (CF) model, parameter identification, stability of time-delay system.**

I. Introduction

TRAFFIC congestion has been one of the most prevalent and stubborn challenges in urban areas for decades, causing a spectrum of issues including wasted time and economic loss [1], elevated driver stress and frustration [2], and increased air pollution [3]. It is estimated that in 2017, traffic congestion costs U.S. more than $300 billion and drivers in big cities spent more than 100 hours in congestion [1]. To alleviate traffic congestion, various traffic control technologies have been proposed, including variable speed limits [4], [5], dynamic traffic light control [6], [7], and ramp metering [8], [9]. It is worth noting that these technologies all require accurate real-time traffic estimation and prediction. It is therefore of critical importance to have good understanding of the traffic flow to enable those traffic control systems.

As such, numerous traffic models have been proposed to investigate traffic characteristics and flow evolution. The traffic models are generally grouped into two categories, macroscopic and microscopic. Macroscopic models are concerned with the macroscopic traffic flow characteristics such as traffic density, average speed, and traffic volume [10]. These traffic models are inspired by continuum fluid flow theories and under different assumptions, they are further classified as kinematic models [11]–[13], dynamic models [14], [15], and lattice hydrodynamic models [16], [17]. On the other hand, microscopic traffic models are concerned with individual vehicles and study the local vehicle interactions in terms of speed, relative distance, and acceleration. Microscopic models can be further categorized as cellular automata (CA) models and car-following (CF) models where CA models are based on stochastic discrete event system with the ability to characterize the lane change behaviors [18], [19] while CF models study the ego vehicle's interaction with its preceding vehicle in a single lane [20], [21]. CF models have great implications to the design of driving assistant systems such as adaptive cruise control [22] and is the focus of this paper.

The development of CF models can date back to the 1950s [20]. Among the many CF models, the arguably most well-known model is the Gazis-Herman-Rothery (GHR) model, which was developed by the General Motors research lab in the late 1950s [21]. The model is based on the hypothesis that the acceleration of the ego vehicle is proportional to the relative speed and inversely proportional to the relative distance, assessed at time τ earlier with τ being the delay due to reaction time. Parameters including the orders of the speed term and relative distance term, as well as a gain, were calibrated using data from wire-linked vehicles. Since then, many variants of GHR models have been developed, proposing different combinations of "optimal" parameters on various sets of experimental data [23]–[25]. Another class of widely-used CF models are the optimal velocity models (also referred to as Helly model), which considers a speed and/or acceleration dependent desired spacing and explicitly incorporates an error term [26]. Several variants have also been proposed and calibrated on different experimental datasets [27], [28]. Besides the above models, some other types of models are also proposed, including collision avoidance

Manuscript received December 24, 2018; revised May 20, 2019; accepted June 21, 2019. This work was supported by the National Natural Science Foundation of China under Grant 61803259 and Grant 61833012. The Associate Editor for this paper was M. Brackstone. *(Corresponding author: Xiang Yin.)*

Z. Li, F. Khasawneh, and A. Li are with the Department of Mechanical Engineering, Michigan State University, East Lansing, MI 48824 USA (e-mail: lizhaoj1@egr.msu.edu; khasawn3@egr.msu.edu; liaoxue@egr.msu.edu).

X. Yin is with the Department of Automation, Shanghai Jiao Tong University, Shanghai 200240, China (e-mail: yinxiang@sjtu.edu.cn).

Z. Song is with the Department of Electrical Engineering and Computer Science, University of Michigan, Ann Arbor, MI 48109 USA (e-mail: ziyou@umich.edu).

Digital Object Identifier 10.1109/TITS.2019.2926146

models [18], [19], psychophysical models [29], [30], and fuzzy logic-based models [31]. A comprehensive review of the CF models can be referred to [22]. Despite the many aforementioned CF models, the available relationships are still not rigorously understood and proven [22].

In this paper, we propose a new microscopic CF model, inspired by the mechanical mass-spring-damper-clutch system. There are natural similarities between the CF dynamics and the mass-spring-damper-clutch system: 1) the ego vehicle tends to accelerate when the relative distance to the lead vehicle is too large and tends to decelerate when the relative distance is too small, which resembles a mechanical spring between two masses; 2) the ego vehicle tends to follow a similar speed as the lead vehicle, resisting large speed difference. This phenomenon resembles a mechanical damper between two masses; 3) drivers tend to have delayed actions due to reaction time, which resembles a mechanical clutch whose engagement induces delays. Therefore, we propose a mass-spring-damper-clutch system to model the CF dynamics. In [32], a mass-spring system is proposed, which is oversimplified and neglects the delayed reaction and resistance to relative speed. A similar mass-spring-damper system was proposed in [33], however, the delay due to the driver's reaction time is also neglected. With the proposed mass-spring-damper-clutch model, we further conduct stability analysis on the time delays and the related parameters using spectral element method [34].

Real-time driving prediction has shown to be critical to improve fuel efficiency and road safety in advanced driving assistant systems [35]. In this study, we develop a parallel recursive least squares with inverse QR decomposition to identify the model parameters in real-time. The algorithm is very computationally efficient and numerically stable that is suitable for the use of real-time prediction [36]. We validate the parameter identification framework in both simulations and naturalistic driving data of three drivers. Promising performance is demonstrated.

The contributions of this paper include the following. First of all, we develop a novel mechanical system inspired mass-spring-damper-clutch system to model the CF dynamics. The new model incorporates the impacts of the ego vehicle on the lead vehicle and can be extended to estimate and predict macroscopic traffic flow with wave propagation techniques on chained mass-spring-damper systems. Secondly, we perform stability analysis on the proposed model using the spectral element method to determine the system parameter set that retains stability under different time delays. Last but not least, we develop a parallel recursive least square with inverse QR decomposition to estimate the model parameters in real time with great computational efficiency and numerical stability. Promising results are demonstrated both in simulations and on naturalistic driving data.

The remainder of this paper is organized as follows. In Section II, we present our mechanical system inspired CF model, followed by the stability analysis of the model in Section III. In Section IV, we present an online parameter identification algorithm using parallel recursive least squares with inverse QR decomposition. The validation of the parameter identification framework is presented in Section V, both in simulation and on experimental data. Finally, conclusion remarks are drawn in Section VII.

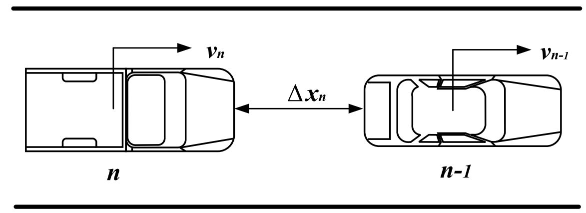

(a) Schematic diagram for car-following dynamics.

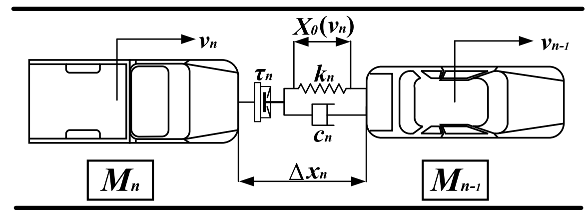

(b) A mechanical mass-spring-damper-clutch system.

Fig. 1. A car following model using a mass-spring-damper-clutch system.

II. Mechanical System Inspired CF Model

The car-following dynamics is illustrated in Figure 1a, where vehicle n follows vehicle $n-1$ in a single lane. By convention, we name vehicle $n-1$ the lead vehicle and vehicle n the follow/ego vehicle. The speeds of the ego vehicle and the lead vehicle are v_n and v_{n-1}, respectively. The relative distance (or range) between the two vehicles is denoted as Δx_n. A car following model is characterized in terms of the ego vehicle's acceleration as a function of relative distance, vehicle speed, and relative vehicle speed [21]:

$$a_n(t) = f(\Delta x(t-\tau_n), \Delta v_n(t-\tau_n), v_n(t-\tau_n)), \qquad (1)$$

where a_n is the acceleration of the ego vehicle (vehicle n), τ_n is the delay due to driver reaction time and vehicle response time of the ego vehicle, and $\Delta v_n = v_{n-1} - v_n$ is the relative speed between the lead vehicle and the ego vehicle. Various mathematical models have been proposed to characterize the relationship [21], [23], [26], [28]. However, these models are mainly based on data regression and lack insights on the system dynamics [22].

In this paper, we propose a new mechanical system inspired CF model as shown in Figure 1b, where vehicle n and vehicle $n-1$ are, respectively, represented as rigid bodies with masses M_n and M_{n-1}. The two masses are connected with a spring with stiffness k_n, a damper with damping coefficient c_n, and a clutch that induces time delay τ_n. Note from the observation that drivers have different desired relative distances at different vehicle speeds [26], [27], the spring in the model has the following speed-dependent relaxation length $X_0(v_n)$, which is illustrated in Figure 2.

$$X_0(v_n) = \begin{cases} X_{0,\min}, & \text{if } v_n < v_{n,1} \\ s_n \cdot v_n, & \text{if } v_{n,1} \le v_n \le v_{n,2} \\ X_{0,\max}, & \text{otherwise,} \end{cases} \qquad (2)$$

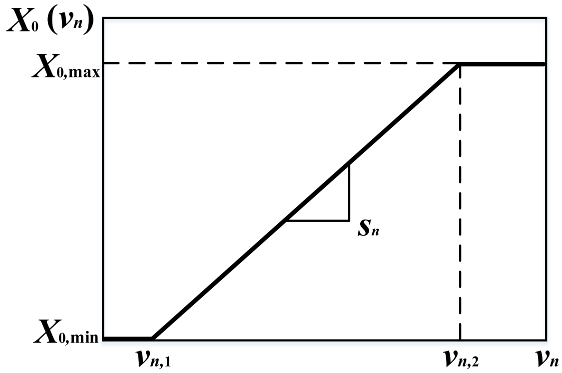

Fig. 2. Speed-dependent spring relaxation length.

where $v_{n,1}$ and $v_{n,2}$ represent the lower and upper threshold points, respectively; and the slope is denoted as s_n.

The mass-spring-damper-clutch system naturally characterizes human driving when following a vehicle. First, drivers tend to resist large relative speed (positive or negative), which is captured by the damper that exerts forces responding to relative speed between the two vehicles. The spring stiffness k_n in the model represents the driver's resistance to the deviation from a desired following distance where larger k_n indicates the driver's stronger preference on maintaining a (speed-dependent) desired following distance. Second, drivers tend to follow a desired speed-dependent distance from the lead vehicle, which is captured by the spring with a speed-dependent relaxation length that exerts forces responding to deviations from the relaxation equilibrium. Larger k_n indicates the driver's stronger preference on maintaining the desired following distance. Third, the delay τ_n due to driver reaction time and vehicle response time is captured by the clutch which induces a time delay for engage and disengage.

Remark 1 (Advantages of the Proposed Model): Compared to existing CF models [21], [23], [24], [26]–[28], the proposed model offers several advantages. First, unlike existing models that are mainly derived from data regression, this mechanical system inspired model provides interpretable physical insights on the CF dynamics. Second, the proposed model can characterize the impact of the ego vehicle on the lead vehicle, i.e., the lead vehicle tends to accelerate (if not changing lane) if the ego vehicle stays too close. This phenomenon is neglected in existing models and therefore it will cause issues when chaining CF models to represent macroscopic traffic. Third, thanks to the wave propagation techniques in mechanical mass-spring systems, the proposed model has good scalability when the mass-spring-damper-clutch systems are chained together to model macroscopic traffic flow, e.g., study the impact of shock waves in the context of mass-spring-damper systems.

Based on the mass-spring-damper-clutch model and the Newton's law, the equations of motion of the system can be written as:

$$\begin{aligned} \Delta\dot{x}_n(t) &= v_{n-1}(t) - v_n(t), \\ M_n\dot{v}_n(t) &= k_n\left[\Delta x_n(t-\tau) - X_0(v_n(t-\tau))\right] \\ &\quad + c_n\Delta v_n(t-\tau). \end{aligned} \tag{3}$$

In a normal highway car-following case, i.e., $v_{n,1} \leq v_n \leq v_{n,2}$, the second equation in (3) becomes

$$\begin{aligned} \dot{v}_n(t) &= k_n/M_n(\Delta x_n(t-\tau) - s v_n(t-\tau)) \\ &\quad + c_n/M_n\,\Delta v_n(t-\tau). \end{aligned} \tag{4}$$

Defining $x_1 = \Delta x_n$, $x_2 = \Delta v_n$, and $u = v_{n-1}$, (3) can be written as

$$\begin{aligned} \dot{x}_1(t) &= u(t) - x_2(t), \\ \dot{x}_2(t) &= k_n/M_n\left[x_1(t-\tau) - s x_2(t-\tau)\right] \\ &\quad + c_n/M_n(u(t-\tau) - x_2(t-\tau)). \end{aligned} \tag{5}$$

In the following section, we investigate the stability of the model on the system parameters and time delay.

III. Stability Analysis

In this section, we perform stability analysis of the proposed CF model in Section II. From (5) and introducing the new variables $\alpha = k_n/M_n$ and $\beta = c_n/M_n$, and setting the lead vehicle's speed to be constant according to $u(t) = u(t-\tau) = u$, equation (5) can then be written as

$$\begin{bmatrix}\dot{x}_1\\ \dot{x}_2\end{bmatrix} = \begin{bmatrix}0 & -1\\ 0 & 0\end{bmatrix}\begin{bmatrix}x_1(t)\\ x_2(t)\end{bmatrix} + \begin{bmatrix}0 & 0\\ \alpha & -(s\alpha+\beta)\end{bmatrix}\begin{bmatrix}x_1(t-\tau)\\ x_2(t-\tau)\end{bmatrix} + \begin{bmatrix}u\\ \beta u\end{bmatrix}, \quad \text{or } \dot{\mathbf{x}} = \mathbf{A}\mathbf{x}(t) + \mathbf{B}\mathbf{x}(t-\tau) + \mathbf{f}(t), \tag{6}$$

where A, B, and f are corresponding matrices. Equation (6) is a Delay Differential Equation (DDE) with a constant point delay τ. The state-space for these equations is typically taken as the space of continuous functions. Consequently, due to the infinite dimensional nature of this state-space the stability analysis of Eq. (6) is more difficult than its delay-free counterpart. Nonetheless, there are several methods available for the stability analysis of this problem including the semi-discretization method [37], Chebyshev polynomials [38], and the spectral element method (SEM) [34]. In this paper we will use the SEM approach due to its flexibility and efficiency [39].

The main idea of the SEM is to discretize the state space of Eq. (6) and then construct a dynamic map over one period where the length of this period for autonomous systems is typically taken to be the length of the time delay τ. The eigenvalues of the resulting matrix that describes this dynamic map must be within the unit disc of the complex plan in order for the corresponding DDE to be stable. While convergence in the SEM can be obtained either by using multiple temporal elements (h-refinement) or by increasing the order of the interpolating polynomial (p-refinement), in this study we use one temporal element and only increase the order of the polynomials to achieve convergence.

Since the vector $\mathbf{f}$ in Eq. (6) only affects the steady state solution but does not affect the stability analysis, we drop it from the subsequent discussion. Let $\mathbf{T} = \{t_i\}_{i=1}^{n+1}$ be a set of $n+1$ distinct temporal mesh points on $[0, \tau]$, and let $\mathbf{c}_m$ and $\mathbf{c}_{m-1}$ be $2 \times (n+1)$ vectors containing the values of the states $\mathbf{x}(t)$ and the delayed states $\mathbf{x}(t-\tau)$, respectively, evaluated on $\mathbf{T}$. We choose a barycentric Lagrange interpolation [38] to represent the states according to

$$\mathbf{x}(t) = \boldsymbol{\Phi}\,\mathbf{c}_m, \text{ and } \mathbf{x}(t-\tau) = \boldsymbol{\Phi}\,\mathbf{c}_{m-1}, \tag{7}$$

This article has been accepted for inclusion in a future issue of this journal. Content is final as presented, with the exception of pagination.

where $\boldsymbol{\Phi} = \boldsymbol{\Phi}(t) = (\boldsymbol{\phi}(t) \otimes \mathbf{I})$, and $\boldsymbol{\phi}(t)$ is the vector of barycentric Lagrange interpolating polynomials $\boldsymbol{\phi}(t) = [L_1(t), L_2(t), \ldots, L_{n+1}(t)]$, $\mathbf{I}$ is the 2×2 identity matrix, while $\otimes$ is the Kronecker product. We now substitute the state approximations into the DDE to obtain

$$(\dot{\boldsymbol{\Phi}} - \mathbf{A}\boldsymbol{\Phi})\mathbf{c}_m = \mathbf{B}\boldsymbol{\Phi}\mathbf{c}_{m-1} + \boldsymbol{\epsilon}, \tag{8}$$

where $\boldsymbol{\epsilon}$ is the vector of approximation errors. Let $\boldsymbol{\psi} = [\psi_1(t), \psi_2(t), \ldots, \psi_{n+1}(t)]$ be a vector of linearly independent test functions. This set of functions is then used in a Galerkin approach where the errors are required to be perpendicular to the space spanned by the set $\boldsymbol{\psi}$. The result is the $2(n+1) \times 2(n+1)$ system of equations

$$\left(\int_0^\tau \boldsymbol{\Psi}\left(\dot{\boldsymbol{\Phi}} - \mathbf{A}\,\boldsymbol{\Phi}\right)dt\right)\mathbf{c}_m = \left(\int_0^\tau \boldsymbol{\Psi}\,\mathbf{B}\,\boldsymbol{\Phi}\,dt\right)\mathbf{c}_{m-1}, \tag{9}$$

where $\boldsymbol{\Psi} = (\boldsymbol{\psi} \otimes \mathbf{I})^T$. Note that the integrals in Eq. (9) are often difficult to evaluate analytically which necessitates using numerical integration as described in [34]. Equation (9) can then be used to construct a dynamic map $\boldsymbol{\Gamma}$ according to

$$\begin{aligned}\mathbf{c}_m &= \left(\int_0^\tau \boldsymbol{\Psi}\left(\dot{\boldsymbol{\Phi}} - \mathbf{A}\,\boldsymbol{\Phi}\right)dt\right)^{-1}\left(\int_0^\tau \boldsymbol{\Psi}\,\mathbf{B}\,\boldsymbol{\Phi}\,dt\right)\mathbf{c}_{m-1} \\ &= \boldsymbol{\Gamma}\mathbf{c}_{m-1}.\end{aligned} \tag{10}$$

In order to ascertain the stability of Eq. (6), we examine the eigenvalues of $\boldsymbol{\Gamma}$: if all the eigenvalues are within a modulus of less than one in the complex plane then the system is asymptotically stable.

In this paper we used the SEM with a 100×100 grid in the (α, β) plane where $\alpha \in [0.01, 2]$, $\beta \in [0.01, 8]$, while 6 equally spaced values of τ were considered in the range $\tau \in [0.2, 2]$. The temporal mesh used consisted of 21 Legendre-Gauss-Lobatto points which correspond to an interpolating polynomial of order 20, while the trial functions were the shifted Legendre polynomials. Increasing the order of the interpolating polynomial beyond 20 did not change the results, thus indicating the convergence of the solution.

Figure 3 shows the stability diagram in the (α, β) plane for 6 different values of τ. The shaded region under each curve is stable, while the area above the curves are unstable. It can be seen that the triangular stability regions shrink as the value of the delay parameter increases from 0.2 to 2. In order to show the resulting stable and unstable system responses two points were simulated in Figs. 3b and c using Matlab's dde23 function and a value of $u = 20$ in Eq. (6). The chosen stable point is $(\alpha = 1, \beta = 2, \tau = 0.2)$, while the selected unstable point is $(\alpha = 1.6, \beta = 2, \tau = 0.2)$. The history function used in the simulation was the perturbed steady state solution $\tilde{\mathbf{x}} = \mathbf{x}_{\text{stst}}(1 + 0.10)$ where $\mathbf{x}_{\text{stst}}$ is the constant steady state solution given by

$$\mathbf{x}_{\text{stst}} = \begin{bmatrix} x_1 \\ x_2 \end{bmatrix}_{\text{stst}} = \frac{u}{\alpha}\begin{bmatrix} -1 + \alpha s + \beta \\ \alpha \end{bmatrix}. \tag{11}$$

Figure 3b shows that the perturbed system goes back to the steady state solution as the system evolves. In contrast,

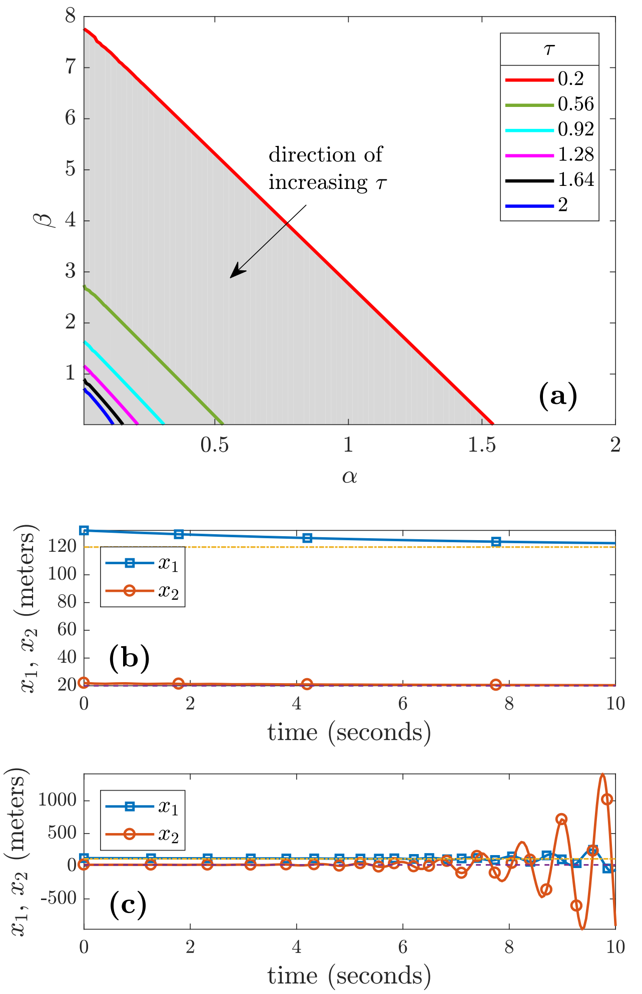

Fig. 3. (a) The stability diagram in the (α, β) plane for increasing values of τ as well as the simulated time series for $\tau = 0.2$, (b) $(\alpha = 1, \beta = 2)$, and (c) $(\alpha = 1.6, \beta = 2)$.

the perturbed, unstable system of Fig. 3c deviates from the steady state solution and grows exponentially.

IV. Online Parameter Identification

Vehicle speed prediction is essential in automated longitudinal control for improved fuel efficiency and safety [35]. Existing studies on cooperative cruise control generally assume that the dynamics of the preceding vehicles are available [40], [41]. While this assumption is valid for fully autonomous vehicle platoon, it does not hold if human drivers are involved. Therefore, it is important to accurately predict human driver maneuvers to provide a "comprehensive preview". In this paper, we develop a framework to identify the parameters and predict vehicle speed changes online.

We first discretize (4) using the explicit Euler method with sampling time Δt, which gives

$$\begin{aligned}\frac{v_n(k) - v_n(k-1)}{\Delta t} &= k_n/M_n(\Delta x_n(k-d) - s_n v_n(k-d)) \\ &\quad + c_n/M_n\,\Delta v_n(k-d),\end{aligned} \tag{12}$$

where $d = \text{round}(\tau_n/\Delta t)$ is the corresponding delayed steps.

For a specific delay d, define $\alpha_n(d) = k_n/M_n$, $\beta_n(d) = -(k_n s_n)/M_n$, and $\gamma_n(d) = c_n/M_n$, then (12) can be written as the following linear equation:

$$[\Delta x_n(k-d)\ v_n(k-d)\ \Delta v_n(k-d)] \begin{bmatrix} \alpha_n(d) \\ \beta_n(d) \\ \gamma_n(d) \end{bmatrix} = \frac{v_n(k)-v_n(k-1)}{\Delta t}. \quad (13)$$

Given a time series data of K steps, $K > d$, and define the parameter vector $p_n(d) = [\alpha_n(d); \beta_n(d); \gamma_n(d)]$, then the parameters can be identified by solving the following least-square problem:

$$\min_{p_n(d)} \|A_n(d)p_n(d) - B_n(d)\|^2, \quad (14)$$

where

$$A_n(d) = \begin{bmatrix} \Delta x_n(0) & v_n(0) & \Delta v_n(0) \\ \Delta x_n(1) & v_n(1) & \Delta v_n(1) \\ \vdots & \vdots & \vdots \\ \Delta x_n(N-d) & v_n(N-d) & \Delta v_n(N-d) \end{bmatrix}$$

and

$$B_n(d) = \frac{1}{\Delta t} \cdot \begin{bmatrix} v_n(d) - v_n(d-1) \\ v_n(d+1) - v_n(d) \\ \cdots \\ v_n(N) - v_n(N-1) \end{bmatrix}$$

are the data matrices of vehicle n. Note that for different delay ds, the data matrices are different, which leads to different identified parameters. In this paper, we consider the possible range of the delay $\tau_n \in [\tau_{\min}, \tau_{\max}]$. With the sampling time Δt, the range of the discrete time delay is $d \in \{d_{\min}, d_{\min}+1, \cdots, d_{\max}\}$, where $d_{\min} = round(\tau_{\min}/\Delta t)$ and $d_{\max} = round(\tau_{\max}/\Delta t)$.

It is straightforward to show that the optimal solution to (14) is

$$p_n^*(d) = (A_n^{\mathrm{T}}(d)A_n(d))^{-1}A_n^{\mathrm{T}}(d)B_n(d). \quad (15)$$

Note that the sizes of matrices A_n and B_n increase as the data length grows, causing computational issues if implemented online. Therefore, recursive computation is needed. In this paper, we exploit a recursive least squares with inverse QR decomposition algorithm (RLS-IQR) for online identification, which has great numerical stability and computational efficiency [36]. Specifically, at each time step k, $k > d$, the algorithm takes in the input vector $x(k) = [\Delta x_n(\text{k-d})\ \ v_n(k-d)\ \ \Delta v_n(k-d)]$ and output $y(k) = \frac{v_n(k)-v_n(k-1)}{\Delta t}$, and then update the parameters $p_n(d)$. The details of the update is shown in Algorithm 1. Since there are multiple possible delays, we run the RLS-IQR in parallel for each $d \in \{d_{\min}, d_{\min}+1, \cdots, d_{\max}\}$. To determine the best delay d and the corresponding parameter $p_n^*(d)$ for prediction, we accumulate the prediction error as:

$$J(d, k+1) = (1-\alpha_0)J(d,k) + \alpha_0|y(k+1) - x(k+1)p_n^*(d)|, \quad (16)$$

with $J(d, 0) = 0$ for all $d \in \{d_{\min}, d_{\min}+1, \cdots, d_{\max}\}$ and $\alpha_0 \in (0, 1]$ is the learning rate. To determine the best delay

Algorithm 1 Parallel Recursive Least Squares With Inverse QR Decomposition

Parameters: Accumulated error learning rate α_0, RLS forgetting factor λ, inverse matrix initialization parameter δ.
Inputs : $\{\Delta x_n(k), v_n(k), \Delta v_n(k)\}_{k=1}^N$.
Outputs : $\{p_n(d,k), J_n(d,k)\}_{k=1}^N$, $d = d_{\min}, \cdots, d_{\max}$.

initialize $p_n(d,0) \leftarrow \mathbf{0}_{3\times 1}$, $R^{-\mathrm{T}}(d) \leftarrow \delta\mathbf{I}_3$, $J(d,0) \leftarrow 0$, $d = d_{\min}, \cdots, d_{\max}$;
for $k = 1 \to N$ **do**
  /* *Parallel loop for possible delays* */
  for $d = d_{\min} \to d_{\max}$ **do**
    if $k \geq d$ **then**
      set $x^{\mathrm{T}}(k) \leftarrow [\Delta x_n(k-d)\ v_n(k-d)\ \Delta v_n(k-d)]$, $y^{\mathrm{T}}(k) \leftarrow \frac{v_n(k)-v_n(k-1)}{\Delta t}$;
      /* *Accumulate prediction error* */
      compute $e_d(k|k-1) = y(k) - x^{\mathrm{T}}(k)p_n(d,k)$;
      $J(d,k) \leftarrow (1-\alpha)J(d,k-1) + \alpha|e_d(k|k-1)|$;
      /* *Parameter update* */
      initialize $u_{j,m} \leftarrow 0, b_0 \leftarrow 1, 1 \leq j \leq 3,\ m < j$;
      for $i = 1 \to 3$ **do**
        $a_i = \lambda^{-1/2}\sum_{j=1}^{i} r_{ij}(d,k-1)x_k(j)$;
        $b_i = \sqrt{b_{i-1}^2 + a_i^2}$;
        $s_i = a_i/b_i$;
        $c_i = b_{i-1}/b_i$;
        for $j = 1 \to i$ **do**
          $r_{ij}(k) = \lambda^{-1/2}c_i r_{ij}(k-1) - s_i u_{i-1,j}$;
          $u_{i,j} = c_i u_{i-1,j} + \lambda^{-1/2}s_i r_{ij}(k-1)$;
        end
      end
      $z(k) = e(k|k-1)/b_3$;
      for $i = 1 \to 3$ **do**
        $p_n(d,k) \leftarrow p_n(d,k-1) + z(k)u_{i,3}$;
      end
    end
  end
end

parameter d, we use the delay parameter corresponding to the minimum accumulated error:

$$d^*(k) = \arg\min_{d} J(d,k). \quad (17)$$

Then the parameter for prediction is chosen as $p^*(k) = p_n(d^*)$. The process is summarized in Algorithm 1.

V. Simulation Validation

In this section, we perform simulation to validate the developed online parameter identification algorithm. Towards that end, we use the mass-spring-damper-clutch system with the parameters listed in Table I. The vehicle following is simulated over a 50 seconds horizon with initial ego vehicle speed 5 m/s and initial distance headway 20 m. The lead vehicle speed profile is set as $v_l = 15 - 5\exp(-0.05t)$. Following the dynamics (5), the ego vehicle speed and the relative distance

TABLE I
PARAMETERS FOR VEHICLE FOLLOWING SIMULATION

$M_n[kg]$	$k_n[N/m]$	$c_n[N \cdot s/m]$	$s_n[s]$	$\tau_n[s]$	$\Delta t[s]$
1000	100	500	5	0.4	0.1

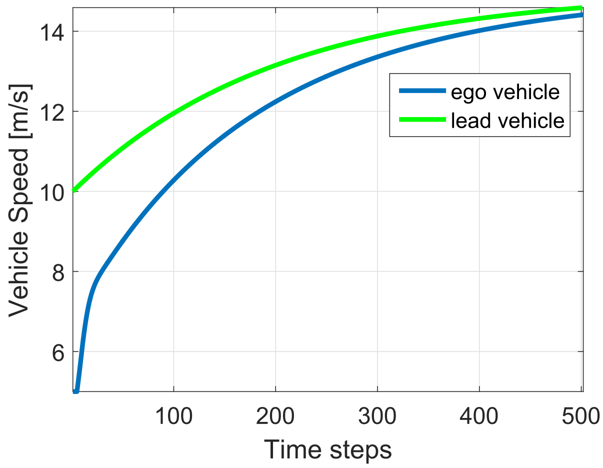

Fig. 4. Simulated vehicle speeds.

is obtained. The speeds of the lead vehicle and ego vehicle are shown in Figure 4.

We apply the Parallel RLS-IQR algorithm in Section IV on the simulated data. We consider the reaction time range as $\tau_{\min} = 0.2[s]$ and $\tau_{\max} = 1[s]$. With the sampling time $\Delta t = 0.1$, the corresponding delays are $d_{\min} = 2$ and $d_{\max} = 10$. As a result, we run a parallel of 9 RLS-IQR for each of the possible delays. The main parameters in the algorithm include the forgetting factor γ , learning rate α_0, and inverse matrix initialization δ. The forgetting factor $0 < \lambda \leq 1$ reduces the influence of old data; one typically chooses a value between 0.9 and 1. It is equivalent to adding exponential weights $e^{-\lambda k}$ for data from k steps back. Our prior experience indicates that 0.95 is a reasonable choice and has thus been used in this study. The learning rate parameter α_0 controls how aggressive the parameters are updated. High α_0 corresponds to faster convergence but too high α_0 can also make the parameter update diverge. In our application, the value 0.05 gives consistently fast convergence rate (10 steps as shown in Fig. 6). The matrix inverse initialization parameter δ is a large positive number. However, too large δ can slow down the convergence rate. Through tuning we find that $\delta = 10$ is a good choice. The accumulated prediction error for all the delays are shown in Figure 5. It can be seen that $d = 4$ gives the lowest prediction error, which matches the specified time delay in the simulation.

The online estimated parameters are shown in Figure 6. It can be seen that in the ideal simulation case, i.e., no model uncertainty and perfect measurement, it only takes 10 steps (1 second) to identify the parameters. This justifies the use of online prediction. However, in reality sensor noises exist in the measurement channel. We next investigate the sensitivity of algorithms to the measurement noises.

Towards this end, we inject measurement noises in the measurement channels. We consider 4 levels of noises with

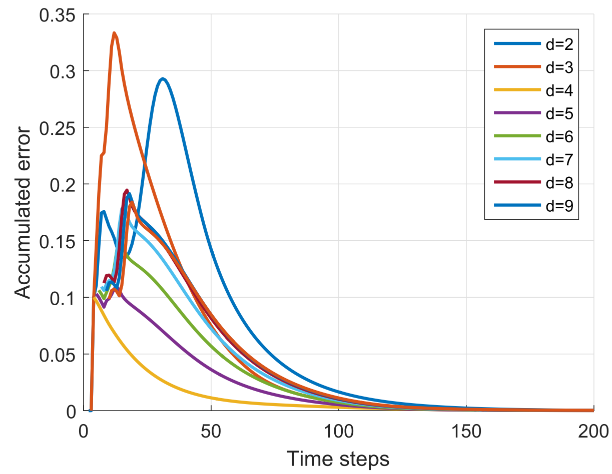

Fig. 5. Accumulated prediction error for possible delays.

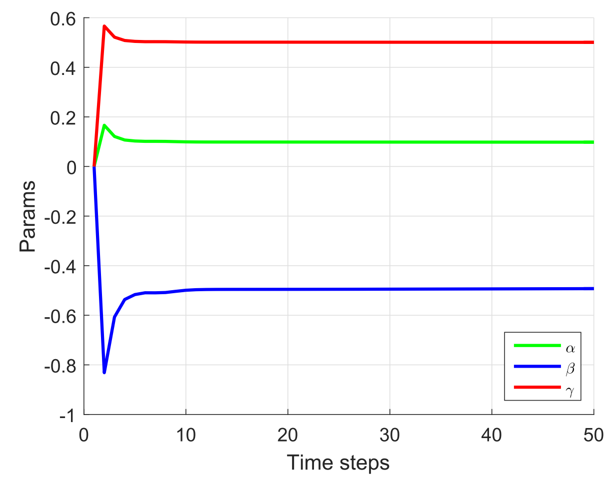

Fig. 6. Online estimated parameters. It can be seen that it only takes 10 steps (1 sec) to correctly identify the parameters in simulation.

respect to signal-to-noise ratio (SNR). The SNR of a discrete signal y of length N with noise e is defined as

$$SNR = 10 \log_{10} \frac{\sum_{k=1}^{N} (y(k) - e(k))^2}{\sum_{k=1}^{N} e^2(k)}. \tag{18}$$

In the simulation, we inject Gaussian noises to ego vehicle speed, relative distance, relative speed, and acceleration of the ego vehicle. We performed the online system identification on noise levels: no noise, SNR 30 dB, SNR 15 dB, and SNR 5 dB. The parameter estimation performance is shown in Figures 7-9. It can be seen that the algorithm is robust to noises and have fast convergence rate even under large noise levels.

Remark 2: The online algorithm described above is used to identify the parameters of the ego car driver that can be used to predict driver demand for engine efficiency. We note that if Vehicle-to-Vehicle (V2V) communication is available, the lead vehicle's car following data (i.e., range, relative speed, and acceleration) can be transmitted to the ego car and the parameters of the lead car can be similarly identified. This prediction can be utilized to improve the controls of the ego car for better fuel efficiency, ride comfort, and safety.

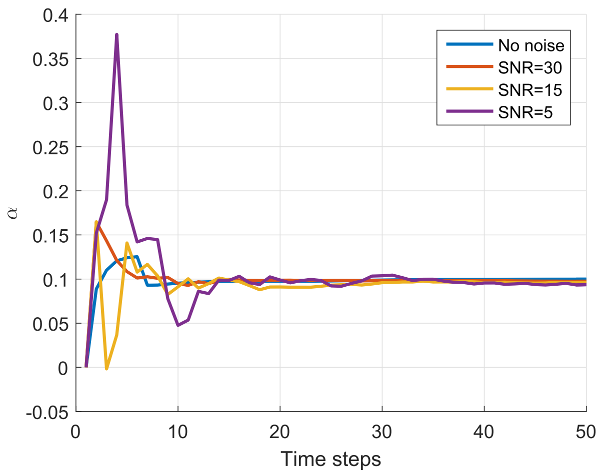

Fig. 7. Estimation of α under different noise levels.

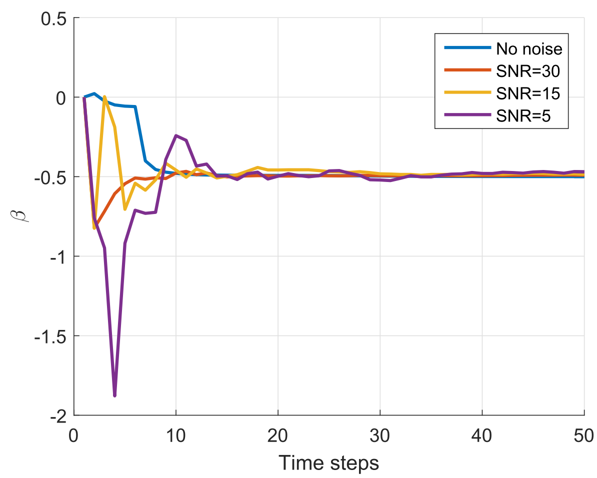

Fig. 8. Estimation of β under different noise levels.

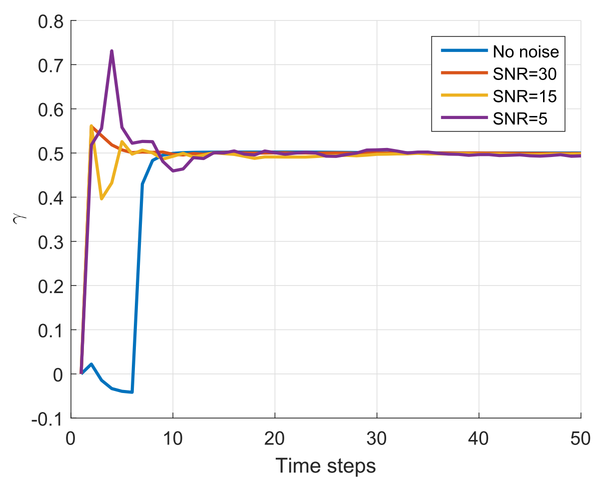

Fig. 9. Estimation of γ under different noise levels.

Furthermore, we study the case where lane changes are involved. Specifically, we consider that a vehicle cuts in between the lead vehicle and the ego vehicle. As shown in Figure 10, at second 10 a vehicle cuts in with a speed less than the previous lead vehicle but greater than the ego vehicle. The relative distance between the cut-in vehicle and the ego vehicle is set as 30 meters. The parameters of the new lead car

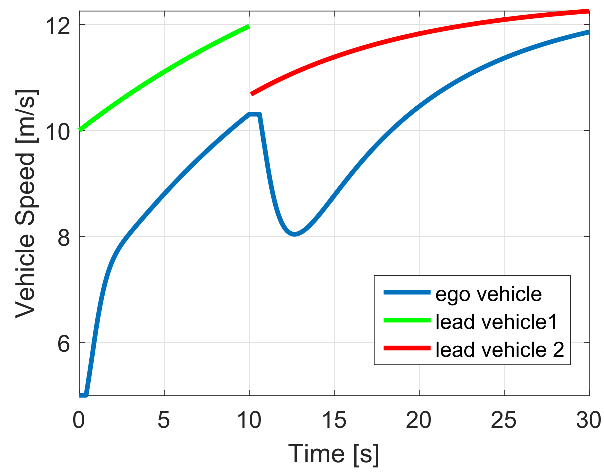

Fig. 10. Simulated vehicle speeds when a vehicle cuts in at 10 sec. The ego vehicle first decelerate to accommodate to the sudden change and then accelerate to similar speed of the lead vehicle.

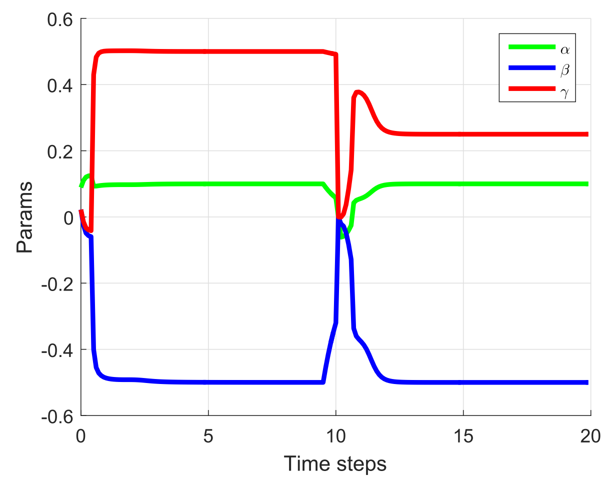

Fig. 11. Online identified parameters when a vehicle cuts in at 10 sec. The parameters resets its values and quickly converges again.

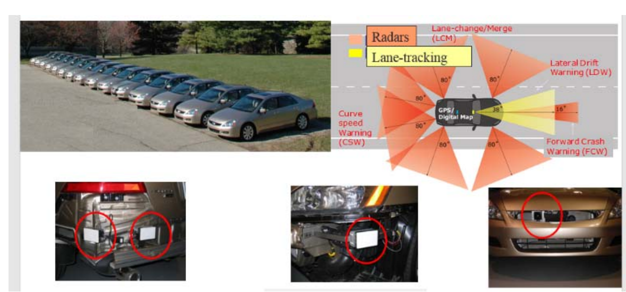

Fig. 12. Vehicle fleet and instrumentation for the IVBSS program.

remains the same except that γ is now set as 0.25. It can be seen that the ego vehicle responds by first decelerating due to reduced relative distance and then accelerate to catch up with the lead vehicle speed. When a lane changing is detected (e.g., the relative distance suddenly changes more than a threshold such as 5 meters), then the parameter identification algorithm resets. It can be seen that the algorithm quickly converges to the new parameters within two seconds. This demonstrates the feasibility of its online implementation even under scenarios with sudden changes.

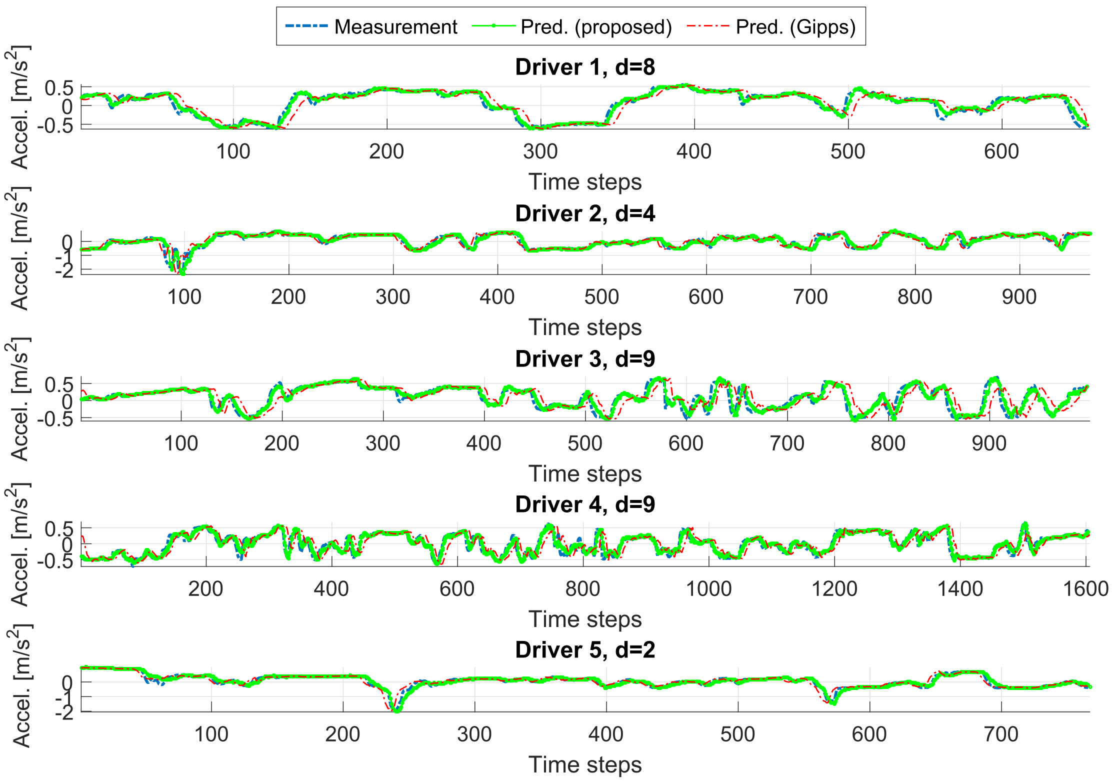

Fig. 13. Sample vehicle acceleration and online predictions for five drivers. The prediction is based on best approximated delays, i.e., the lowest accumulated prediction error. The proposed CF model has better prediction performance than the Gipps model due to its online adaptation capability.

VI. Model Validation on Naturalistic Driving Data

In this section, we validate the proposed mass-spring-damper-clutch CF model and the online parameter estimation algorithm on a naturalistic driving dataset from the Integrated Vehicle based Safety System (IVBSS) program [42]. The main objective of the IVBSS program was to investigate the effectiveness of driving assistant systems such as Lane Departure Warning, Curve Speed Warning, and Forward Crash Warning. A diverse group of 108 drivers participated in the program with balanced age and gender. The participants drove the experimental vehicles for their personal use for about six weeks. The experimental vehicles are equipped with data collection instruments to record driving data including vehicle speed and acceleration, as well as the relative distance and relative speed to the leading vehicle that are estimated using Mobileye [43]. Data including vehicle speed, acceleration, relative distance and relative distance are recorded every 0.1 second (10 Hz). The vehicle fleet and some instrumentations are illustrated in Figure 12.

To validate the proposed model, we use the naturalistic driving data from five randomly selected participants. For each driver, we extract around five car-following episodes where the cruise control is disengaged and there is no relative distance jumps due to lead vehicle lane change or other vehicle cut-ins. We apply the parallel RLS-IQR algorithm for online acceleration prediction for delays varying from 2 steps to 10 steps. The relative distance, vehicle speed, and relative speed are scaled by 1/40, 1/30, and 1/4, respectively to make the three inputs at similar level. To better validate the CF model, we also compare the model with the Gipps CF model [44], which is widely used in traffic simulators. The model predicts the vehicle speed as

$$v_n(t+\tau) = \min\{v_n^{acc}(t+\tau), v_n^{dec}(t+\tau)\}, \qquad (19)$$

with $v_n^{acc} = v_n(t) + 2.5 a_n \tau (1 - v_n(t)/v_n^d)(0.025 + v_n(t)/v_n^d)^{\frac{1}{2}}$ and $v_n^{dec}(t+\tau) = -\tau d_n + (\tau^2 d_n^2 + d_n(2[x_{n-1}(t) - x_n(t) - S_{n-1}] - \tau v_n(t) + v_{n-1}^2(t)/d_{n-1}))^{\frac{1}{2}}$. Here τ again is the reaction time; $v_n(t)$ and v_{n-1} are, respectively, the speeds of follow vehicle and lead vehicle; v_n^d and a_n are the desired speed and maximum acceleration, respectively; d_n and d_{n-1} are respectively the most aggressive braking that the follower wishes to undertake and the estimate of the leader's most severe braking capability; $x_n(t)$ and x_{n-1} are, respectively, the longitudinal position of follow vehicle and lead vehicle; and finally S_{n-1} is the "leader's effective length". For comparison, the delay parameter τ is chosen as the one that gives the best performance when calibrating the proposed CF model. The remaining set of parameters (i.e., a_n, v_n^d, d_n, d_{n-1}, and S_{n-1}) are trained offline using half of the driving data. A sample trajectory and the prediction of the proposed CF model with best estimated delays as well as the Gipps model from each driver is shown in Figure 13. It can be seen that the online prediction offers promising prediction performance, better than the Gipps model due to its capability of online adaptation. The prediction error statistics for the five drivers are listed in Table II. The online identified parameters for driver 1 are shown in Figure 14. We note that the values of γ have high fluctuations, which is an indication of the need

TABLE II
PREDICTION PERFORMANCE SUMMARY

Driver ID	avg. RMSE (proposed)	worst RMSE (proposed)	avg. RMSE (Gipps)	worst RMSE (Gipps)
1	0.28	0.33	0.53	0.7
2	0.32	0.42	0.41	0.65
3	0.26	0.35	0.28	0.42
4	0.46	0.52	0.82	1.07
5	0.42	0.48	0.45	0.72

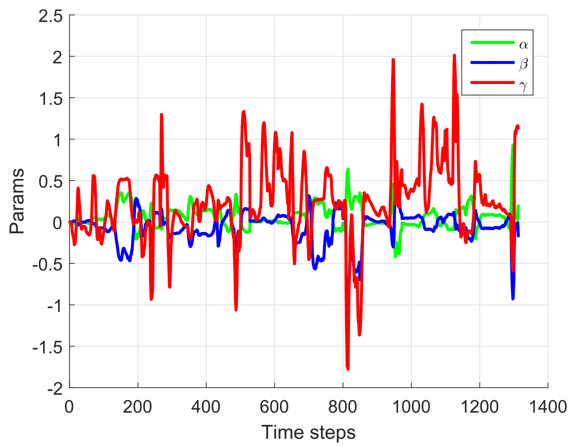

Fig. 14. Online estimated parameters.

of a nonlinear damper to better characterize the CF dynamics. This will be investigated in our future work.

The algorithm is implemented on a standard laptop with the Intel i7-55000U CPU @2.40GHz processor and 8 GB RAM. The average CPU time for one-step update is 0.0535 ms and the worst CPU time for one-step update is 0.0921 ms, indicating the great computational efficiency of the proposed method and the feasibility of the online implementation. We also note that another major advantage of the inverse QR-decomposition based RLS is the numerical stability, which has been demonstrated in several other works [36]. In our work, we also show that the algorithm remains stable in both simulations and naturalistic driving data validations.

VII. CONCLUSION

In this paper, we developed a novel mechanical-system inspired microscopic traffic model using a mass-spring-damper-clutch system. This model naturally captures general CF behaviors and offers physical interpretations of the CF dynamics. It also considers the impact of the following vehicle on the lead vehicle, which is neglected in existing microscopic CF models and causes issues when chaining vehicles for macroscopic traffic modeling. We develop a parallel recursive least square with inverse QR decomposition algorithm for online parameter identification. The parameter identification has been validated in both simulations and on naturalistic driving data with promising performance.

We found that the damper-related parameter has high fluctuations in naturalistic driving data, which is an indication that a nonlinear damper may be needed to improve the CF modeling. Future work will include the consideration of nonlinear spring/damper to further improve the model. We will also chain the vehicles together and study the wave propagation on the vehicle platoons.

REFERENCES

[1] *Inrix Global Traffic Scorecard*, INRIX, Kirkland, WA, USA, 2018.

[2] D. A. Hennessy and D. L. Wiesenthal, "The relationship between traffic congestion, driver stress and direct versus indirect coping behaviours," *Ergonomics*, vol. 40, no. 3, pp. 348–361, Nov. 1997.

[3] K. Zhang and S. Batterman, "Air pollution and health risks due to vehicle traffic," *Sci. Total Environ.*, vols. 450–451, pp. 16–307, Apr. 2013.

[4] E. R. Müller, R. C. Carlson, W. Kraus, and M. Papageorgiou, "Microsimulation analysis of practical aspects of traffic control with variable speed limits," *IEEE Trans. Intell. Transp. Syst.*, vol. 16, no. 1, pp. 512–523, Feb. 2015.

[5] A. Heygi, B. Schutter, and J. Hellendoorn, "Optimal coordination of variable speed limits to suppress shock waves," *IEEE Trans. Intell. Transp. Syst.*, vol. 6, no. 1, pp. 102–112, Mar. 2005.

[6] M. B. Younes and A. Boukerche, "Intelligent traffic light controlling algorithms using vehicular networks," *IEEE Trans. Veh. Technol.*, vol. 65, no. 8, pp. 5887–5899, Aug. 2016.

[7] J. L. Fleck, C. G. Cassandras, and Y. Geng, "Adaptive quasi-dynamic traffic light control," *IEEE Trans. Control Syst. Technol.*, vol. 24, no. 3, pp. 830–842, May 2016.

[8] Y. Wang, E. B. Kosmatopoulos, M. Papageorgiou, and I. Papamichail, "Local ramp metering in the presence of a distant downstream bottleneck: Theoretical analysis and simulation study," *IEEE Trans. Intell. Transp. Syst.*, vol. 15, no. 5, pp. 2024–2039, Oct. 2014.

[9] I. Papamichail and M. Papageorgiou, "Traffic-responsive linked ramp-metering control," *IEEE Trans. Intell. Transp. Syst.*, vol. 9, no. 1, pp. 111–121, Mar. 2008.

[10] C. F. Daganzo, "The cell transmission model, part II: Network traffic," *Transp. Res. B, Methodol.*, vol. 29, no. 2, pp. 79–93, 1995.

[11] P. I. Richards, "Shock waves on the highway, " *Oper. Res.*, vol. 4, no. 1, pp. 42–51, Feb. 1956.

[12] C. F. Daganzo, "A finite difference approximation of the kinematic wave model of traffic flow," *Transp. Res. Part B, Methodol.*, vol. 29, no. 4, pp. 261–276, 1995.

[13] D. Helbing, A. Hennecke, V. Shvetsov, and M. Treiber, "MASTER: Macroscopic traffic simulation based on a gas-kinetic, non-local traffic model," *Transp. Res. B, Methodol.*, vol. 35, no. 2, pp. 183–211, Feb. 2001.

[14] B. S. Kerner and P. Konhäuser, "Cluster effect in initially homogeneous traffic flow," *Phys. Rev. E, Stat. Phys. Plasmas Fluids Relat. Interdiscip. Top.*, vol. 48, pp. R2335–R2338, Oct. 1993.

[15] H.-N. Nguyen, B. Fishbain, E. Bitar, D. Mahalel, and P.-O. Gutman, "Dynamic model for estimating the macroscopic fundamental diagram," *IFAC-PapersOnLine*, vol. 49, no. 3, pp. 297–302, 2016.

[16] R. Kaur and S. Sharma, "Analyses of a heterogeneous lattice hydrodynamic model with low and high-sensitivity vehicles," *Phys. Lett. A*, vol. 382, no. 22, pp. 1449–1455, Jun. 2018.

[17] H. X. Ge, R. J. Cheng, and L. Lei, "The theoretical analysis of the lattice hydrodynamic models for traffic flow theory," *Phys. A, Stat. Mech. Appl.*, vol. 389, no. 14, pp. 2825–2834, 2010.

[18] E. Kometani and T. Sasaki, "Dynamic behaviour of traffic with a nonlinear spacing-speed relationship," in *Proc. Symp. Theory Traffic Flow*, 1959, pp. 105–119.

[19] P. G. Gipps, "A behavioural car-following model for computer simulation," *Transp. Res. B, Methodol.*, vol. 15, no. 2, pp. 105–111, 1981.

[20] L. A. Pipes, "An operational analysis of traffic dynamics," *J. Appl. Phys.*, vol. 24, no. 3, pp. 274–281, 1953.

[21] D. Gazis, R. Herman, and R. Rothery, "Nonlinear follow-the-leader models of traffic flow," *Oper. Res.*, vol. 9, no. 4, pp. 545–567, Aug. 1961.

[22] M. Brackstone and M. McDonald, "Car-following: A historical review," *Transp. Res. F, Traffic Psychol. Behavior*, vol. 2, no. 4, pp. 181–196, 1999.

[23] R. Herman and R. B. Potts, "Single lane traffic theory and experiment," in *Proc. Symp. Theory Traffic Flow*. Amsterdam, The Netherlands: Elsevier, 1959, pp. 147–157.

[24] A. May and H. Keller, "Non-integer car-following models," *Highway Res. Rec.*, vol. 199, no. 1, pp. 19–32, 1967.

[25] H. Ozaki, "Reaction and anticipation in the car following behavior," in *Proc. 13th Int. Symp. Traffic Transp. Theory*, 1993, pp. 349–366.

[26] W. Helly, "Simulation of bottlenecks in single lane traffic flow," in *Proc. Symp. Traffic Transp. Theory*, 1959, pp. 207–238.

[27] M. Aron, "Car following in an urban network: Simulation and experiments," in *Proc. Seminar D, 16th PTRC Meeting*, 1988, pp. 27–39.

[28] J. Xing, "A parameter identification of a car-following model," in *Proc. 2nd World Congr. (ATT)*, 1995, pp. 1739–1745.

[29] R. Michaels, "Perceptual factors in car following," in *Proc. 2nd Int. Symp. Theory Road Traffic*, 1963, pp. 44–59.

[30] L. Evans and R. Rothery, "Experimental measurement of perceptual thresholds in car following," *Highway Res. Rec.*, vol. 64, pp. 13–29, Aug. 1973.

[31] C. Kikuchi and P. Chakroborty, "Car following model based on a fuzzy inference system," *Transp. Res. Rec.*, vol. 65, no. 13, pp. 82–91, 1992.

[32] Y. Li, W. Chen, S. Peeta, X. He, T. Zheng, and H. Feng, "An extended microscopic traffic flow model based on the spring-mass system theory," *Mod. Phys. Lett. B*, vol. 31, no. 9, 2017, Art. no. 1750090.

[33] T.-H. Yang and C.-W. Zu, "Linear dynamic car-following model," in *Proc. 5th World Congr. Intell. Control Automat.*, vol. 6, Jun. 2004, pp. 5212–5216.

[34] F. A. Khasawneh and B. P. Mann, "A spectral element approach for the stability analysis of time-periodic delay equations with multiple delays," *Commun. Nonlinear Sci. Numer. Simul.*, vol. 18, no. 8, pp. 2129–2141, Aug. 2013.

[35] J. I. Ge and G. Orosz, "Connected cruise control among human-driven vehicles: Experiment-based parameter estimation and optimal control design," *Transp. Res. C, Emerg. Technol.*, vol. 95, pp. 445–459, Oct. 2018.

[36] S. T. Alexander and A. L. Ghimikar, "A method for recursive least squares filtering based upon an inverse QR decomposition," *IEEE Trans. Signal Process.*, vol. 41, no. 1, p. 20, Jan. 1993.

[37] T. Insperger and G. Stépán, "Updated semi-discretization method for periodic delay-differential equations with discrete delay," *Int. J. Numer. Methods Eng.*, vol. 61, no. 1, pp. 117–141, Aug. 2004.

[38] E. A. Butcher, H. Ma, E. Bueler, V. Averina, and Z. Szabo, "Stability of linear time-periodic delay-differential equations via Chebyshev polynomials," *Int. J. Numer. Methods Eng.*, vol. 59, no. 7, pp. 895–922, Jan. 2004.

[39] D. J. Tweten, G. M. Lipp, F. A. Khasawneh, and B. P. Mann, "On the comparison of semi-analytical methods for the stability analysis of delay differential equations," *J. Sound Vibrat.*, vol. 331, no. 17, pp. 4057–4071, Aug. 2012.

[40] G. Orosz, "Connected cruise control: Modelling, delay effects, and nonlinear behaviour," *Vehicle Syst. Dyn.*, vol. 54, no. 8, pp. 1147–1176, 2016.

[41] G. Orosz, R. E. Wilson, and G. Stépán, "Traffic jams: Dynamics and control," *Phys. Eng. Sci.*, vol. 368, no. 1928, pp. 4455–4479, 2010.

[42] J. Sayer *et al.*, "Integrated vehicle-based safety systems field operational test final program report," Univ. Michigan Transp. Syst., Ann Arbor, MI, USA, Tech. Rep. DOT HS 811 482, 2011.

[43] G. P. Stein, E. Rushinek, G. Hayun, and A. Shashua, "A computer vision system on a chip: A case study from the automotive domain," in *Proc. IEEE Comput. Soc. Conf. Comput. Vis. Pattern Recognit.*, Sep. 2005, p. 130.

[44] L. Vasconcelos, L. Neto, S. Santos, A. B. Silva, and Á. Seco, "Calibration of the Gipps car-following model using trajectory data," *Transp. Res. Procedia*, vol. 3, pp. 952–961, Apr. 2014.

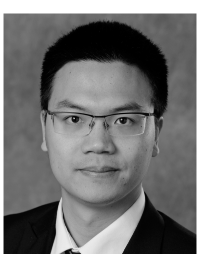

Zhaojian Li received the B.S. degree in civil aviation from the Nanjing University of Aeronautics and Astronautics, Nanjing, China, in 2010, and the M.S. and Ph.D. degrees from the Department of Aerospace Engineering, University of Michigan, Ann Arbor, MI, USA, in 2014 and 2016, respectively. From 2010 to 2012, he was an Air Traffic Controller with the Shanghai Area Control Center, Shanghai, China. From 2014 to 2015, he was an Intern with Ford Motor Company, Dearborn, MI, USA. He is currently an Assistant Professor with the Department of Mechanical Engineering, Michigan State University. His current research interests include optimal control, autonomous vehicles, and intelligent transportation systems.

Firas Khasawneh received the B.S. degree in mechanical engineering from the Jordan University of Science and Technology, Irbid, Jordan, in 2004, the M.S. degree in mechanical and aerospace engineering from the University of Missouri, Columbia, in 2007, and the Ph.D. degree in mechanical engineering from Duke University, Durham, NC, USA, in 2010. From 2011 to 2013, he was a Visiting Assistant Professor with the Pratt School of Engineering, Duke University. From 2013 to 2017, he was with the SUNY Polytechnic Institute, Utica, NY, USA, as an Assistant Professor of mechanical engineering. He joined the Mechanical Engineering Department, Michigan State University, as an Assistant Professor. His current research interests include complex and delayed dynamical systems, time series analysis, machine learning, nonlinear dynamics, and machining dynamics.

Xiang Yin was born in Anhui, China, in 1991. He received the B.Eng. degree from Zhejiang University in 2012, and the M.S. and Ph.D. degrees from the University of Michigan, Ann Arbor, in 2013 and 2017, respectively, all in electrical engineering.

Since 2017, he has been with the Department of Automation, Shanghai Jiao Tong University, where he is currently an Associate Professor. His research interests include formal methods, control of discrete-event systems, model-based fault diagnosis, security, and their applications to cyber and cyber-physical systems. He received the Outstanding Reviewer Awards from *Automatica*, the IEEE TRANSACTIONS ON AUTOMATIC CONTROL, and the *Journal of Discrete Event Dynamic Systems*. He is the Co-Chair of the IEEE CSS Technical Committee on Discrete Event Systems.

Aoxue Li received the B.S. and M.S. degrees in vehicle engineering from Jiangsu University, Zhenjiang, China, in 2013 and 2016, respectively, where he is currently pursuing the Ph.D. degree in vehicle engineering. Since 2018, he has been a Visiting Scholar with the Department of Mechanical Engineering, Michigan State University. His research interests include the autonomous vehicle, intelligent transportation systems, and ADAS technologies.

Ziyou Song received the B.E. degree (Hons.) and the Ph.D. degree (Hons.) in automotive engineering from Tsinghua University, Beijing, China, in 2011 and 2016, respectively. He currently holds a post-doctoral position with the University of Michigan, Ann Arbor. His research interests include battery parameter estimation, hybrid energy storage systems, and electric and hybrid electric vehicles.